Noncovalent, Site-Specific Biotinylation of Histidine-Tagged Proteins

Annett Reichel,[†] Dirk Schaible,[†] Natalie Al Furoukh,[†] Mati Cohen,[‡] Gideon Schreiber,[‡] and Jacob Piehler*,[†]

Institute of Biochemistry, Johann Wolfgang Goethe-University, Frankfurt/Main, Germany, and Department of Biological Chemistry, The Weizmann Institute of Science, Rehovot, Israel

Site-specific conjugation of proteins to surfaces, spectroscopic probes, or other functional units is a key task for implementing biochemical assays. The streptavidin−biotin interaction has proven a highly versatile tool for detection, quantification, and functional analysis of proteins. We have developed an approach for site-specific reversible biotinylation of recombinant proteins through their histidine tag using biotin conjugated to the multivalent chelator trisnitrilotriacetic acid (^{BT}tris-NTA). Stable binding of ^{BT}tris-NTA to His-tagged proteins was demonstrated, which is readily reversed by addition of imidazole, enabling versatile conjugation schemes in solution as well as at interfaces. Gel filtration experiments revealed that His-tagged proteins bind to streptavidin doped with ^{BT}-tris-NTA in a 2:1 stoichiometry. Furthermore, an increased binding affinity toward His-tagged proteins was observed for ^{BT}tris-NTA linked to streptavidin compared to tris-NTA in solution and on surfaces. These results indicate an efficient cooperative interaction of two adjacent tris-NTA moieties with a single His-tag, yielding an extremely tight complex with a lifetime of several days. We demonstrate several applications of ^{BT}tris-NTA including multiplexed capturing of proteins to biosensor surfaces, cell surface labeling, and Western blot detection. The remarkable selectivity of the His-tag-specific biotinylation, as well as the highly stable, yet reversible complex provides the basis for numerous further applications for functional protein analysis.

The high-affinity, selective recognition of biotin by avidin and streptavidin has been applied with great success for numerous bioanalytical purposes, such as protein immobilization on solid supports, protein labeling with spectroscopic probes, and protein detection.[1−3] The versatility of the biotin−streptavidin system relies on (i) the robust, quasi-irreversible interaction, (ii) the multivalent nature of streptavidin, which enables sandwich-type assays, and (iii) the compatibility of biotin with chemical conjugation protocols. One critical issue, however, is the selective, site-specific incorporation of biotin into proteins. Enzymatic transfer of biotin onto an acceptor peptide tag by the BirA protein has been successfully applied,[4] but these schemes proved rather inefficient for in situ biotinylation of proteins, e.g., on the surface of live cells.[5] Recently, more efficient approaches for site-specific covalent biotinylation have been reported,[6−9] yet noncovalent, reversible biotinylation would further increase the versatility of the system, because the biotin−streptavidin interaction can only be reversed under very harsh conditions. Ideally, site-specific biotinylation through a standard affinity tag would be possible. The oligohistidine tag (His-tag) is currently the most generically applied affinity tag for purification and detection of proteins through transition metal ions complexed by chelators such as nitrilotriacetic acid (NTA).[10] NTA-immobilized transition metal ions proved particularly rewarding for selective and site-specific capturing of proteins to surfaces.[11−15] Manipulation of His-tagged proteins in solution, however, was hampered by the low intrinsic affinity of the Ni−NTA complex to the His-tag ($K_D \sim 10\ \mu M$). In order to overcome this drawback, we have developed recognition units with multiple NTA moieties, which bind the His-tag with much higher affinities,[16] which have been successfully applied for functional protein immobilization on surfaces.[17−19] In particular the tris-NTA

* Corresponding author, Phone +49 (0)69 79829468. Fax +49 (0)69 79829495. E-mail: j.piehler@em.uni-frankfurt.de.

[†] Johann Wolfgang Goethe-University.

[‡] The Weizmann Institute of Science.

(1) Wilchek, M.; Bayer, E. A. *Anal. Biochem.* **1988**, *171*, 1−32.
(2) Wilchek, M.; Bayer, E. A. *Trends Biochem. Sci.* **1989**, *14*, 408−412.
(3) Diamandis, E. P.; Christopoulos, T. K. *Clin. Chem.* **1991**, *37*, 625−636.
(4) Beckett, D.; Kovaleva, E.; Schatz, P. J. *Protein Sci.* **1999**, *8*, 921−929.
(5) Chen, I.; Howarth, M.; Lin, W.; Ting, A. Y. *Nat. Methods* **2005**, *2*, 99−104.
(6) Keppler, A.; Gendreizig, S.; Gronemeyer, T.; Pick, H.; Vogel, H.; Johnsson, K. *Nat. Biotechnol.* **2003**, *21*, 86−89.
(7) George, N.; Pick, H.; Vogel, H.; Johnsson, N.; Johnsson, K. *J. Am. Chem. Soc.* **2004**, *126*, 8896−8897.
(8) Yin, J.; Straight, P. D.; McLoughlin, S. M.; Zhou, Z.; Lin, A. J.; Golan, D. E.; Kelleher, N. L.; Kolter, R.; Walsh, C. T. *Proc. Natl. Acad. Sci. U.S.A.* **2005**, *102*, 15815−15820.
(9) Zhou, Z.; Cironi, P.; Lin, A. J.; Xu, Y.; Hrvatin, S.; Golan, D. E.; Silver, P. A.; Walsh, C. T.; Yin, J. *ACS Chem. Biol.* **2007**.
(10) Ueda, E. K.; Gout, P. W.; Morganti, L. *J. Chromatogr., A* **2003**, *988*, 1−23.
(11) Busch, K.; Tampe, R. *J. Biotechnol.* **2001**, *82*, 3−24.
(12) Dorn, I. T.; Pawlitschko, K.; Pettinger, S. C.; Tampe, R. *Biol. Chem.* **1998**, *379*, 1151−1159.
(13) Gershon, P. D.; Khilko, S. *J. Immunol. Methods* **1995**, *183*, 65−76.
(14) Nieba, L.; Nieba-Axmann, S. E.; Persson, A.; Hamalainen, M.; Edebratt, F.; Hansson, A.; Lidholm, J.; Magnusson, K.; Karlsson, A. F.; Pluckthun, A. *Anal. Biochem.* **1997**, *252*, 217−228.
(15) Sigal, G. B.; Bamdad, C.; Barberis, A.; Strominger, J.; Whitesides, G. M. *Anal. Chem.* **1996**, *68*, 490−497.
(16) Lata, S.; Reichel, A.; Brock, R.; Tampé, R.; Piehler, J. *J. Am. Chem. Soc.* **2005**, *127*, 10205−10215.
(17) Tinazli, A.; Piehler, J.; Beuttler, M.; Guckenberger, R.; Tampe, R. *Nat. Nanotechnol.* **2007**, *2*, 220−225.
(18) Tinazli, A.; Tang, J.; Valiokas, R.; Picuric, S.; Lata, S.; Piehler, J.; Liedberg, B.; Tampe, R. *Chemistry* **2005**, *11*, 5249−5259.
(19) Lata, S.; Piehler, J. *Anal. Chem.* **2005**, *77*, 1096−1105.

10.1021/ac0714922 CCC: $37.00
Published on Web 10/23/2007

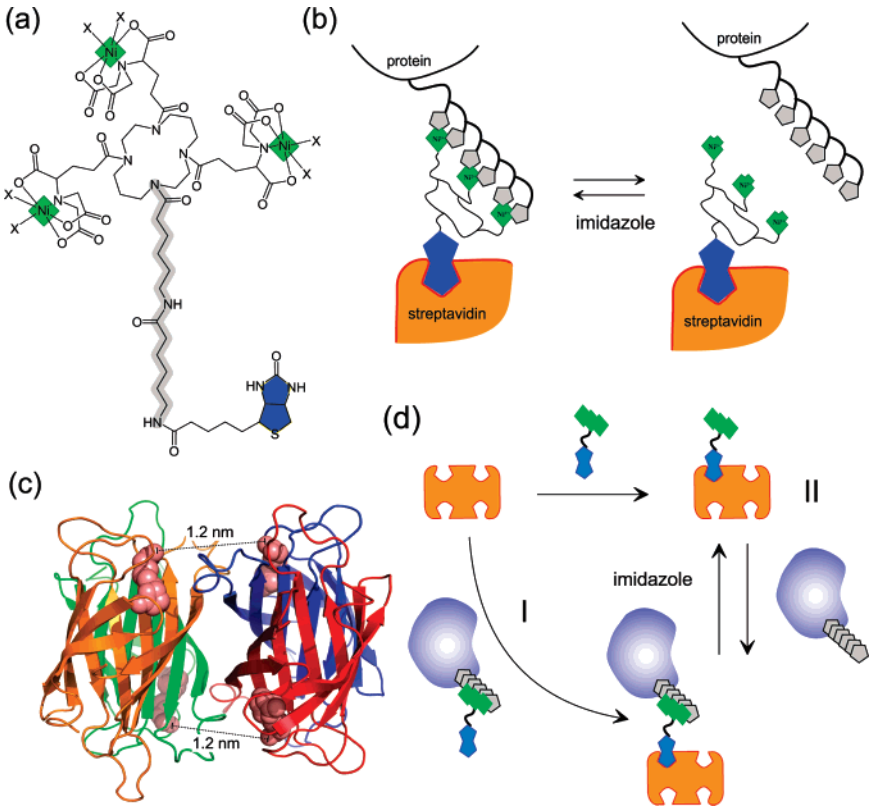

Figure 1. Concept of the ^{BT}tris-NTA adaptor function. (a) Chemical structure of ^{BT}tris-NTA loaded with Ni(II) ions. (b) Principle of the reversible biotinylation of histidine-tagged proteins. (c) Structure of streptavidin in complex with four biotin molecules[23] (PDB entry 1STP). (d) Possible schemes of conjugating His-tagged proteins with streptavidin. (I) Biotinylation of a protein by binding of ^{BT}tris-NTA to the His-tag followed by attachment to streptavidin; (II) functionalization of streptavidin with ^{BT}tris-NTA, followed by binding of the His-tagged protein.

adaptor based on a circular scaffold (cf. Figure 1a) very efficiently matches the His-tag, yielding binding affinities in the subnanomolar regime.[16] In contrast to other multivalent NTA heads,[20,21] tris-NTA forms stable, quantitative complexes with His-tagged proteins with a lifetime of several hours,[16] which can be readily isolated by size exclusion chromatography (SEC). For this reason, tris-NTA/fluorophore conjugates have been successfully employed for specifically labeling His-tag proteins in complex matrixes such as bacterial lysates and the surface of live cells.[22]

Here, we have synthesized a novel adaptor for linking His-tagged proteins to the streptavidin world. Biotin was conjugated to tris-NTA through a bisamidocaproic acid linker (Figure 1a).

This adaptor was used for tethering proteins to streptavidin in solution and on different types of surfaces employed for label-free biosensor studies. Owing to the high-affinity, yet fully reversible interaction between tris-NTA and His-tag (Figure 1b), different schemes for conjugation could be applied (Figure 1d). The stoichiometries and the affinities of the protein complexes were explored in detail, and several applications for protein immobilization, labeling and detection are presented.

MATERIALS AND METHODS

Synthesis and Purification of ^{BT}tris-NTA. ^{BT}tris-NTA was synthesized as in principle described previously for other tris-NTA conjugates.[22] Briefly, deprotected tris-NTA with an aminocaproic acid spacer was dissolved in DMF and reacted with a 1.5 stoichiometric excess of biotin−aminohexanoic acid *N*-hydroxylsuccinimide ester (Sigma-Aldrich). The product was precipitated by addition of diethyl ether and purified by reversed-phase HPLC on a C_{18} column (Vydac 218TP54, water/acetonitrile with 0.1% TFA). After HPLC, the pH in the fractions was adjusted by adding 1 M Hepes pH 7.5 to a final concentration of 100 mM. After removal of the volatiles, the product was dissolved in 20−50 mL of MilliQ water to a final concentration of 2−5 mM Hepes pH 7.5, and 5 mM final concentration nickel(II) chloride was added in order to load the NTA head groups. The solution was loaded onto a 1-mL anion-exchange column (Hitrap Q, GE Healthcare) and eluted with a gradient of 0−600 mM sodium chloride. The chelator concentrations were determined photometrically from the Ni(II) absorption at 390 nm using a Ni(II)/NTA solution for calibration.

Protein Expression and Purification. Maltose binding protein with C-terminal hexahistidine (MBP-H6) and decahistidine (MBP-H10) tags were cloned by linker insertion into the multiple cloning site of the vector pMALc2x (New England Biolabs). The proteins were expressed in *Escherichia coli* and purified by immobilized metal affinity chromatography followed by SEC as described previously.[19] The proteins were labeled with Oregon Green 488 (OG488) and ATTO 565 *N*-hydroxysuccinimidyl esters

(20) Kapanidis, A. N.; Ebright, Y. W.; Ebright, R. H. *J. Am. Chem. Soc.* **2001**, *123*, 12123−12125.
(21) Huang, Z.; Park, J. I.; Watson, D. S.; Hwang, P.; Szoka, F. C., Jr. *Bioconjugate Chem.* **2006**, *17*, 1592−1600.
(22) Lata, S.; Gavutis, M.; Tampé, R.; Piehler, J. *J. Am. Chem. Soc.* **2006**, *128*, 2365−2372.
(23) Weber, P. C.; Ohlendorf, D. H.; Wendoloski, J. J.; Salemme, F. R. *Science* **1989**, *243*, 85−88.

in HBS (20 mM Hepes, pH 7.5, 150 mM sodium chloride) according to standard protocols, and the labeled protein was separated from the free dye and aggregates by SEC. The concentrations of protein and the reactive dye were optimized so that an average labeling degree of ~1 was obtained for both proteins. For cysteine-specific, covalent biotinylation of MBP F391 within the linker region between the MBP and the H10-tag was mutated into a cysteine by ligase chain reaction. The protein was expressed in *E. coli* and purified by immobilized metal affinity chromatography as the wild-type. After addition of DTT, the protein was subjected to SEC, followed by reaction with a 2-fold molar excess of *N*-biotinoyl-*N'*-(6-maleimidohexanoyl)hydrazide in HBS according to standard protocols. The biotinylated protein was separated from the free biotin and aggregates by SEC.

The β-lactamase TEM1 and its inhibitor protein BLIP were expressed in *E. coli* as reported previously.[24] The H6- and H10-tags were inserted at the N-terminus of TEM1 (without secretion leader sequence) and BLIP by PCR. TEM1-H10, BLIP-H10, and BLIP-H6 as well as the tagless mutants; TEM1 E104A and BLIP F142A were refolded from inclusion bodies and purified as described previously.[24] Interferon α2 S136C (IFNα2) was expressed, purified, and site-specifically labeled with OG488 (^{OG488}-IFNα2) as described previously.[25]

Size Exclusion Chromatography. Protein complexes were purified and analyzed by SEC on Superdex 200 HR10/300 and PC 3.1/300 columns (both from GE Healthcare) in HBS buffer. His-tagged proteins (10−20 μM) were incubated with a 2-fold concentration of ^{BT}tris-NTA for 15 min and injected on a Superdex 200 HR10/300 column. For dual color detection at 280and 560 nm or 490 nm, measurements were carried out with a Superdex 200 PC 3.2/30 column in a SMART system (GE Healthcare).

Total Reflection X-ray Fluorescence Analysis (TXRF). The amount of Ni(II) ions bound to ^{BT}tris-NTA-loaded streptavidin was determined by TXRF using an EXTRA IIA (Atomica Instruments). Streptavidin loaded with an excess of ^{BT}tris-NTA was purified by SEC on Superdex 200 HR10/300 in Tris−acetate buffer pH 7.5. A total of 36 μL of the purified protein complex (10−20 μM) was mixed with 4 μL of Cr-standard (10 mg/mL), and 4 μL of this sample was placed on a silica substrate. After evaporation of the solvent, the sample was analyzed by TXRF (Mo Kα excitation, 1000-s measurement time).

Reflectance Interference Spectroscopy (RIfS). Protein immobilization and protein interactions were monitored by label-free detection using RIfS. This technique detects binding on the surface of a thin silica interference layer.[26] A home-built setup based on a commercially available diode array spectrometer as described before[27] was used. Binding curves were obtained from the shift of the interference spectrum. A shift of 1 nm corresponds to ~1 ng/mm^2 protein on the surface.[28] Measurements were carried out in HBS supplemented with 0.01% Triton X100 in a flow chamber under continuous flow-through conditions with a data acquisition rate of 1 Hz as described before.[29] The silica surface of the transducer was silanized by reaction with glycidyloxipropyltriethoxysilane (Fluka), followed by reaction with a 1:4 v/v mixture of Boc-NH-OEG$_6$-NH$_2$ and N$_3$-OEG$_6$-NH$_2$ (both from Polypure) according to published protocols.[17,30] The Boc-protected amino groups on the surface were deprotected by incubation for 4 h in trifluoroacetic acid containing traces of water. After washing with water, Biotin−aminohexanoic acid *N*-hydroxysuccinimide ester (Sigma) was coupled in DMF for 15 min at room temperature.

Surface Plasmon Resonance (SPR). Label-free interaction studies by SPR were carried out in a Biacore T100 (GE Healthcare) and a Biorad ProteOn XPR36 system (Biorad). All binding experiments were carried out in HBS supplemented with 0.01% surfactant P20 (GE Healthcare). Biacore experiments were carried out with a streptavidin-functionalized surface (sensor chip SA, GE Healthcare). For functionalization, 1 μM ^{BT}tris-NTA was injected on a single flow channel for 200 s. Subsequently, all samples injected over this channel and an adjacent flow channel for referencing. MBP-H10 was injected at a concentration of 500 nM for 200 s. For correction of the background signals, blank runs were carried out, where buffer was injected instead of the protein solution.

Multiplexed binding experiments were carried out in a ProteOn XPR36 system, where 36 detection spots can be addressed by 6 channels, which can be switched between two perpendicular directions. Measurements were carried out at 25 °C in HBS supplemented with 0.01% Tween on a NeutrAvidin-covered sensor chip (NLC, Biorad) at a flow rate of 30 μL/min. Different concentrations of ^{BT}tris-NTA were injected for 6 min, followed by protein immobilization. Two different BLIP proteins and one TEM1 protein at a 1 μM concentration were injected in parallel on four channels: BLIP-H10 (1 μM), BLIP-H10 (1 μM) mixed with crude *E. coli* lysate, BLIP-H6 (1 μM), and TEM1-H10 (1 μM). Analyte binding was studied with the mutants TEM1 E104A and BLIP F142A at three different concentrations injected perpendicular to the direction of immobilization. For varying the surface concentrations of tris-NTA, ^{BT}tris-NTA was injected in parallel at different concentrations (200, 100, 50, 25, and 12.5 nM). Association and dissociation rate constants (k_a and k_d) were determined by monoexponential fit to the association and dissociation phases.

Stopped-Flow Fluorescence Spectroscopy. Stopped-flow measurements were carried out at SF-61, DX2 Double Mixing Stopped-Flow System (Hi-Tech Scientific) at 26 °C in HBS pH 7.5 supplemented with 1 mg/mL BSA. Complexes of ^{OG488}MBP−H10/H6 with ^{AT565}tris-NTA, or ^{AT565}streptavidin loaded with ^{BT}tris-NTA complexes were purified via size exclusion chromatography and chased with imidazole (50−400 mM in HBS/BSA). ^{OG488}MBP-H10/H6 (25 nM) were excited by a Xe lamp at 480 nm, and the fluorescence dequenching upon complex dissociation was detected through a band-pass filter (500−570 nm).

Cell Culture, Quantum Dot Labeling, and Confocal Fluorescence Microscopy. The gene of ifnar2 without a signal sequence and truncated after the transmembrane domain was cloned into the pDisplay vector (Invitrogen) between the *Bgl*II and the *Pst*I restriction sites followed by an insertion of an N-terminal H10-tag as a linker into the *Bgl*II site. The resulting

(24) Albeck, S.; Schreiber, G. *Biochemistry* **1999**, *38*, 11−21.
(25) Gavutis, M.; Lata, S.; Lamken, P.; Müller, P.; Piehler, J. *Biophys. J.* **2005**, *88*, 4289−4302.
(26) Piehler, J.; Brecht, A.; Gauglitz, G.; Maul, C.; Grabley, S.; Zerlin, M. *Biosens. Bioelectron.* **1997**, *12*, 531−538.
(27) Schmitt, H. M.; Brecht, A.; Piehler, J.; Gauglitz, G. *Biosens. Bioelectron.* **1997**, *12*, 809−816.
(28) Hanel, C.; Gauglitz, G. *Anal. Bioanal. Chem.* **2002**, *372*, 91−100.
(29) Piehler, J.; Schreiber, G. *Anal. Biochem.* **2001**, *289*, 173−186.
(30) Piehler, J.; Brecht, A.; Valiokas, R.; Liedberg, B.; Gauglitz, G. *Biosens. Bioelectron.* **2000**, *15*, 473−481.

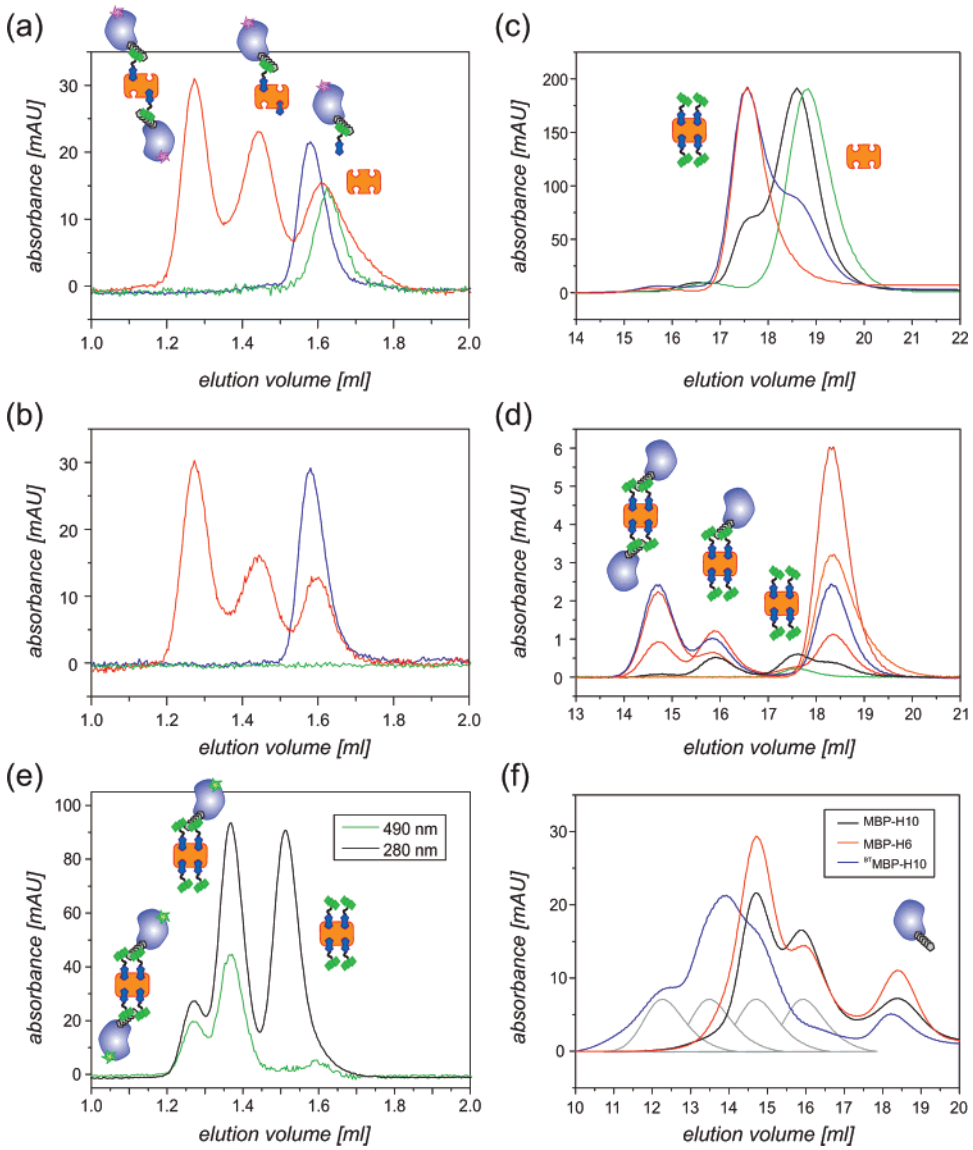

Figure 2. Tethering of His-tagged MBP to streptavidin through ^{BT}tris-NTA analyzed by analytical SEC. (a, b) Binding of ^{AT565}MBP-H10/^{BT}tris-NTA to streptavidin as determined by separation on a Superdex 200 PC 3.2/30 column at 280 (a) and 560 nm (b) (green, streptavidin alone; blue, ^{AT565}MBP-H10/^{BT}tris-NTA; red, streptavidin mixed with ^{AT565}MBP-H10/^{BT}tris-NTA). (c) Loading of streptavidin with ^{BT}tris-NTA at different molar ratios of streptavidin/^{BT}tris-NTA (green, 1:0; black, ~1:1; blue, ~1:3; red, ~1:10) as analyzed on a Superdex 200 HR 10/300 column. (d) Binding of MBP-H10 to streptavidin/^{BT}tris-NTA at different ratios as detected on a Superdex 200 HR 10/300 column at 280 nm. (e) Binding of ^{OG488}MBP-H10 to an excess of streptavidin/^{BT}tris-NTA as detected on a Superdex 200 PC 3.2/30 column at 280 (black) and 490 nm (green). (f) Comparison of the streptavidin/^{BT}tris-NTA complexes with MBP-H10 (black) and MBP-H6 (red) with the complexes obtained with streptavidin and ^{Bt}MBP-H10 (blue) as analyzed on a Superdex 200 HR 10/300 column (the gray peaks indicate the deconvoluted peak positions).

vector was transiently transfected into HeLa cells grown on 24-mm coverslips. A total of 48 h after transfection, the coverslips were mounted into a perfusion cell, incubated with 200 nM ^{BT}-tris-NTA in serum-free culture medium for 15 min, and washed twice with serum-free culture medium. Subsequently, 1 nM Qdot 655 streptavidin conjugate (Quantum Dot Corp., Hayward, CA) was added and incubated for 15 min, followed by treatment with 100 nM ^{OG488}IFNα2.

Western Blotting. Histidine-tagged proteins were detected by Western blot using ^{BT}tris-NTA. Following SDS-PAGE (12% acrylamide), proteins were transferred to a nitrocellulose membrane by electroblotting (20% v/v methanol in SDS running buffer, 6 mA, 90 min). The membrane was blocked with 3% w/v bovine serum albumin and 20 μg/mL avidin in 20 mM Tris pH 8, 250 mM NaCl for 1 h with gentle rocking. The membrane was washed with 20 mM Tris pH 8, 250 mM NaCl, 0.1% (v/v) Tween 20 (2 × 10 mL, 15-min incubation/wash) with gentle rocking and incubated with 25 nM ^{BT}tris-NTA in 10 mL in the same buffer for 15−60 min. After washing with TBST (2 × 10 mL, 15-min incubation/wash), the membrane was incubated with a streptavidin/horsh radish peroxidase conjugate (IBA GmbH, Göttingen, Germany) in 10 mL of TBST (1:20000) for 1 h and washed with TBST (2 × 10 mL, 15-min incubation/wash). The membrane was developed by the addition of enhanced chemiluminescence solution A (5 mL) and solution B (5 mL) (Pierce) and the chemiluminescent signal measured after 1 min in a LumiImager (Roche) with a scan time of 30 s.

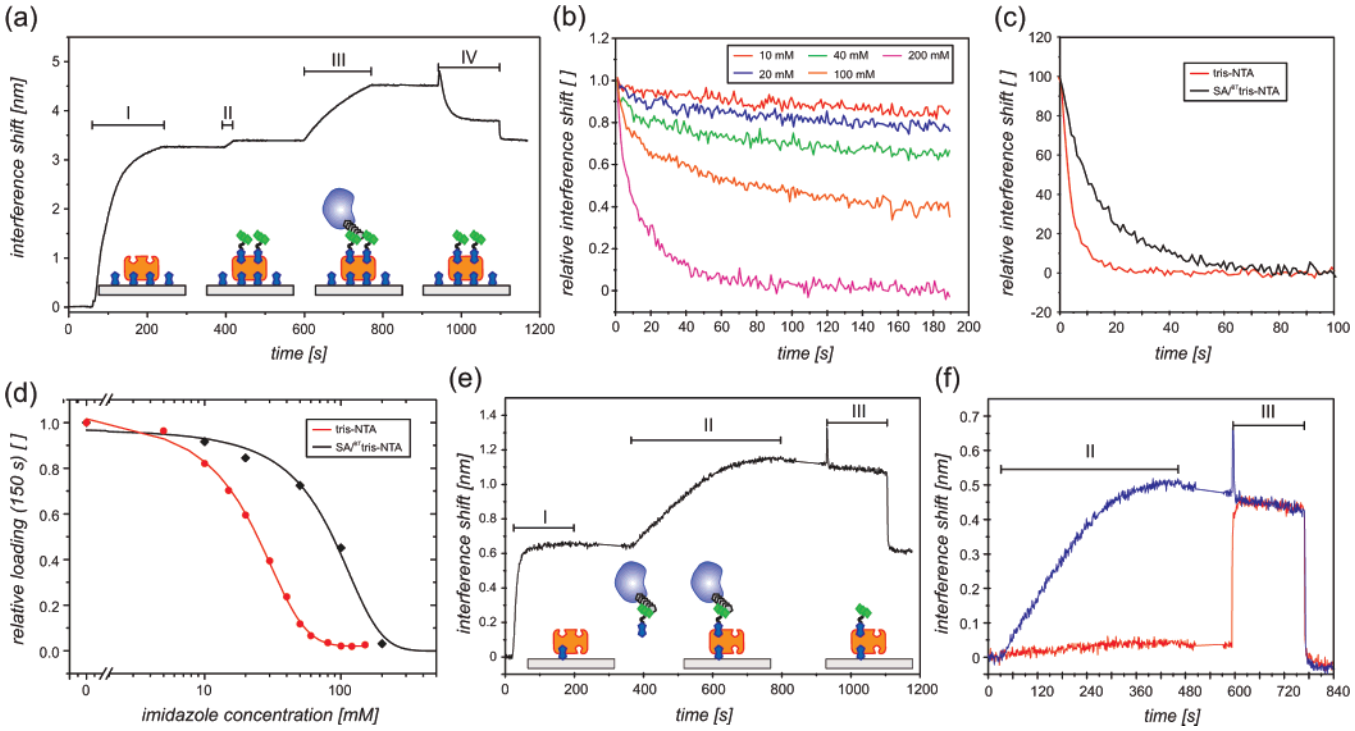

Figure 3. Protein immobilization on streptavidin-functionalized surfaces probed in real time by RIfS. (a) Immobilization of streptavidin on a biotin-functionalized surface (I), loading with ^{BT}tris-NTA (II), binding of MBP-H10 (III), and elution with imidazole (IV) as detected by RIfS. (b) Dissociation kinetics of MBP-H10 during rinsing with imidazole at different concentrations. (c) Dissociation kinetics of MBP-H10 at 200 mM imidazole from ^{BT}tris-NTA-loaded streptavidin (SA/ ^{BT}tris-NTA) compared with the dissociation from conventional tris-NTA functionalized surfaces under the same conditions. (d) Comparison of the imidazole titration curves for MBP-H10 interaction with covalently coupled tris-NTA and ^{BT}tris-NTA loaded onto streptavidin surfaces (SA/^{BT}tris-NTA): The relative signal after 150 s rinsing with imidazole at different concentrations is plotted. (e) Direct capturing of 10 nM MBP-H10 in complex with ^{BT}tris-NTA (II) after loading the surface with streptavidin (I), followed by regeneration with imidazole (III). (f) Comparison of the binding kinetics of 10 nM MBP-H10/^{BT}tris-NTA to streptavidin (blue line) and 10 nM MBP-H10 to streptavidin saturated with ^{BT}tris-NTA (red line). Note that during injection of imidazole, a background signal of ~0.45 nm is observed due to changes in the refractive index.

RESULTS AND DISCUSSION

^{BT}tris-NTA Stably Links His-Tagged Proteins to Streptavidin in Solution. The different schemes of conjugating His-tagged proteins with streptavidin through the ^{BT}tris-NTA adaptor (cf. Figure 1d) were first explored by analytical SEC using maltose-binding protein with a C-terminal decahistidine-tag (MBP-H10), which was amine-specifically labeled with ATTO565 (^{ATTO565}MBP-H10) for selective detection. ^{ATTO565}MBP-H10 was conjugated with a 2-fold molar excess of ^{BT}tris-NTA, and the complex was purified by SEC. The biotinylated ^{AT565}MBP-H10 was subsequently incubated with streptavidin, and the complexes were separated by SEC using dual color detection at 280 and 560 nm (Figure 2a,b). Two additional distinct peaks were observed for this mixture. From the ratio of the signals at 280 nm and at 560 nm, a 1:2 ratio of ^{AT565}MBP-H10 can be estimated for these complexes. This result, as well as the shift of the peaks indicates formation of 1:1 and 1:2 complexes between streptavidin and ^{AT565}MBP-H10. This could be explained by steric hindrance, which may prohibit docking of two MBP-H10 to the two ^{BT}tris-NTA, which are in proximity (cf. Figure 1c). However, it could also be that both adjacent ^{BT}tris-NTA moieties are involved in the interaction with one His-tag, and therefore, only two MBP-H10 molecules can bind to one streptavidin molecule.

We furthermore explored the alternative pathway for ^{BT}tris-NTA-mediated conjugation of His-tagged proteins with streptavidin (cf. Figure 1d, path II) by SEC. Upon binding of ^{BT}tris-NTA to streptavidin, a substantial shift of the streptavidin peak to higher molecular mass was observed (Figure 2c), which is probably due to the rather high hydrodynamic ratio of the tris-NTA moiety.[16] In the case of substoichiometric amounts of ^{BT}tris-NTA, further peaks were observed, the number of which, however, could not be resolved. With an excess of ^{BT}tris-NTA, a single peak was observed, for which the 1:4 stoichiometry of the streptavidin/^{BT}-tris-NTA complex was confirmed by determining the concentration of Ni(II) ions bound to an equivalent of strepavidin by TXRF. When MBP-H10 was added to the purified streptavidin/^{BT}tris-NTA complex, again two addition peaks were obtained, which correspond to 1:1 and 1:2 complexes between streptavidin/^{BT}tris-NTA and MBP-H10 (Figure 2d). Using Oregon Green 488-labeled MBP-H10 (^{OG488}MBP-H10) and dual color detection, quantitative complex formation could be demonstrated (Figure 2e). These experiments confirm that both labeling schemes depicted in Figure 1d can be employed for conjugation streptavidin with His-tagged proteins. The interaction of MBP-H6 with streptavidin/^{BT}tris-NTA yielded the same stoichiometry of the complex compared to MBP-H10 (Figure 2f). In contrast, MBP-H10, which was site-specifically biotinylated through a Cys mutation close to the C-terminal His-tag (^{BT}MBP-H10), additionally formed 3:1 and 4:1 complexes with streptavidin (Figure 2f). These results suggest that the simultaneous interaction of two tris-NTA groups bound to streptavidin with a single His-tagged

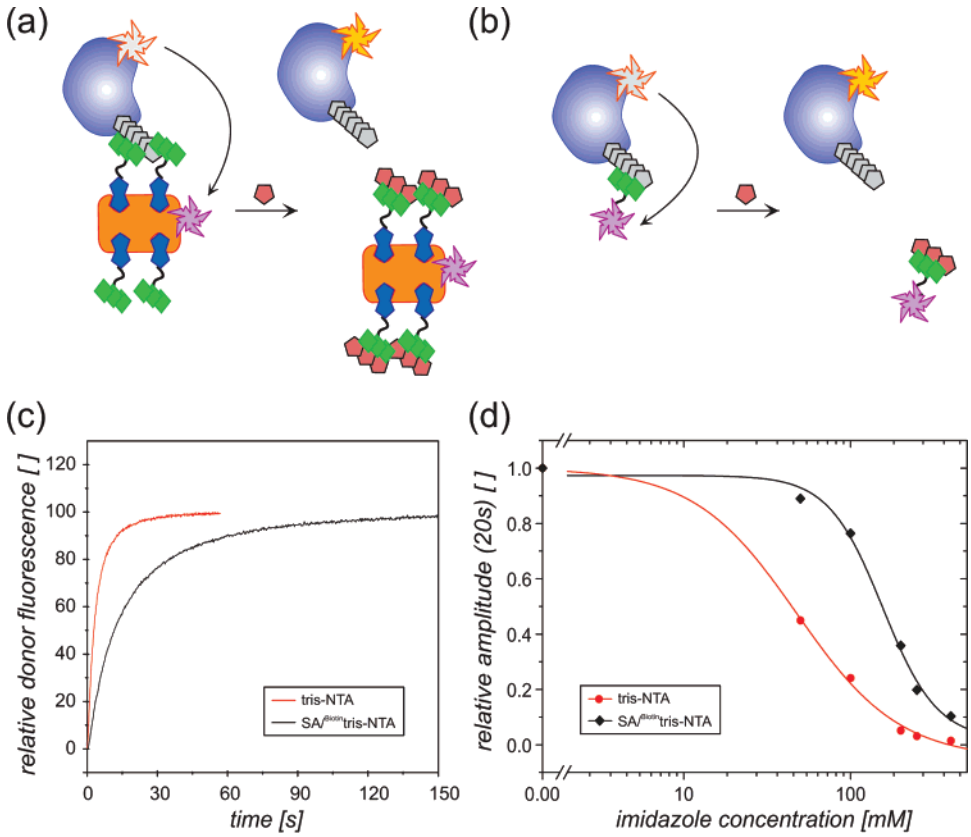

Figure 4. Stability of the complexes in solution. (a, b) Schematic illustration of the assay: ^{OG488}MBP-H10, (c) Dissociation kinetics of ^{AT565}-tris-NTA/^{OG488}MBP-H10 in comparison to ^{AT565}streptavidin/^{BT}tris-NTA/^{OG488}MBP-H10 upon mixing with 200 mM imidazole as detected by stopped-flow fluorescence. (d) Comparison of the imidazole titration curves of the interaction of ^{OG488}MBP-H10 with ^{AT565}tris-NTA and with ^{AT565}streptavidin loaded with ^{BT}tris-NTA.

protein is energetically favorable compared to binding of two His-tagged proteins.

Stable and Versatile Capturing of Proteins to Surfaces. We further explored the interaction and the labeling schemes with ^{BT}tris-NTA by using reflectance interference spectroscopy for label-free, solid-phase detection. Streptavidin was immobilized onto a PEG polymer brush functionalized with biotin, and the remaining biotin binding sites were subsequently loaded with ^{BT}tris-NTA (Figure 3a). When MBP-H10 was loaded onto these surfaces, highly stable binding was observed. The specificity of the interaction was confirmed by the full reversibility upon injection of imidazole. Furthermore, no protein binding was observed in the absence of Ni(II) ions, as well as without loading the streptavidin with ^{BT}tris-NTA (data not shown).

The binding affinity of the interaction between MBP-H10 and the streptavidin/^{BT}tris-NTA was studied by monitoring the imidazole-induced dissociation kinetics at different imidazole concentrations (Figure 3b,c). We observed 4−5-fold slower dissociation from streptavidin/^{BT}tris-NTA than from tris-NTA covalently coupled to a PEG polymer brush.[19] This result is in line with the preferred 1:2 stoichiometry we have observed by SEC, which suggested that simultaneous interaction of one His-tagged protein with two streptavidin-bound tris-NTA is energetically favorable. Also for MBP-H6, efficient capturing and stable binding to streptavidin/^{BT}tris-NTA-functionalized surfaces was observed (data not shown).

We furthermore explored direct immobilization of His-tagged proteins, which were biotinylated through ^{BT}tris-NTA (Figure 3e,f). Fast binding of MBP-H10/^{BT}tris-NTA was observed even at a concentration of 10 nM. In contrast to covalently biotinylated proteins, quantitative elution with 200 mM imidazole was possible. The linear, diffusion-controlled binding kinetics during injection of MBP-H10/^{BT}tris-NTA confirmed efficient biotinylation, since binding with dramatically slower association kinetics was observed when MBP-H10 at the same concentration was binding to streptavidin already saturated with ^{BT}tris-NTA (Figure 3f). This is in line with the rather low association rate constant of the oligohistidine binding to Ni−NTA ($\sim 1 \times 10^5$ $M^{-1}s^{-1}$).

Increased Binding Stability of ^{BT}tris-NTA in Solution. We further explored the enhanced stability of the interaction of MBP-H10 with ^{BT}tris-NTA in complex with streptavidin compared to the tris-NTA/MBP-H10 complex by probing the molecular interaction in solution by Förster resonance energy transfer. For this purpose, complexes of ^{OG488}MBP-H10 with ATTO565-labeled tris-NTA (^{AT565}tris-NTA) as wells as 1:1 complexes of ^{OG488}MBP-H10 with ATTO565-labeled streptavidin (^{AT565}streptavidin) fully loaded with ^{BT}tris-NTA were purified by SEC. Recovery of the OG488 fluorescence upon dissociation of the complex by mixing with imidazole was monitored by stopped-flow fluorescence detection (Figure 4a,b). Again, ~5 times slower dissociation was observed for the complex with ^{AT545}streptavidin/^{BT}tris-NTA compared to ^{AT565}-tris-NTA (Figure 4c,d).

The same stability was observed for the 1:1 and the 1:2 complexes of streptavidin/^{BT}tris-NTA/MBP-H10, confirming binding to two independent sites. These results support that both tris-

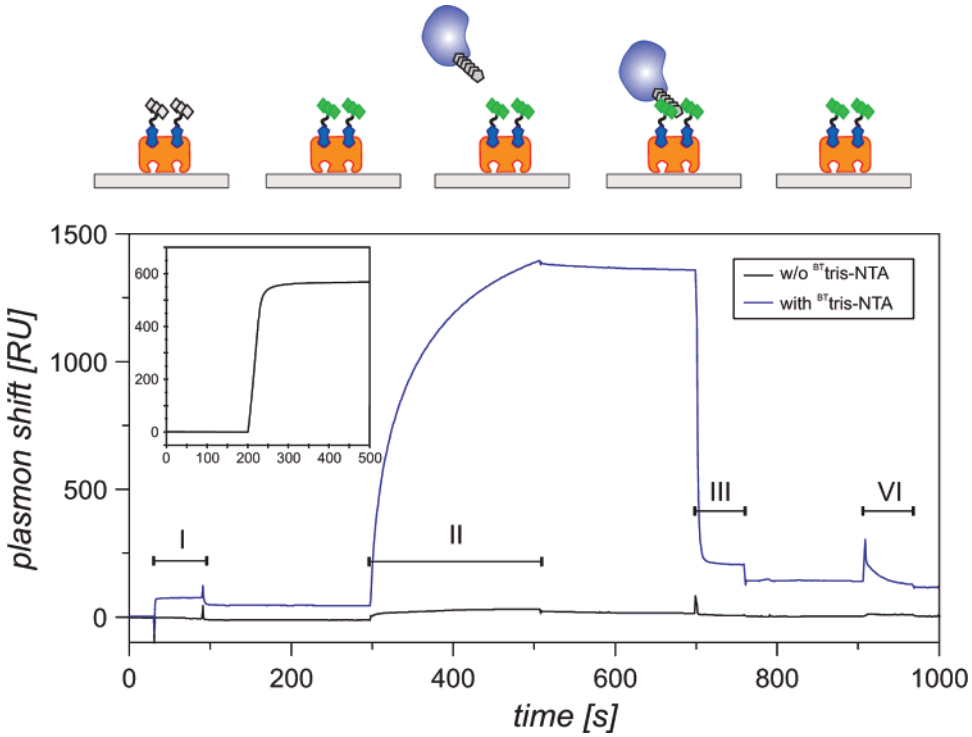

Figure 5. Reversible capturing of proteins onto a commercial BIAcore chip. A sensor chip SA was loaded with 500 nM ^{BT}tris-NTA on one channel (inset), and all metal ions were removed by injection of 200 mM EDTA (not shown). Subsequently, 10 mM nickel(II) chloride (injection I) followed by 500 nM MBP-H10 (injection II) were injected on two channels. Immobilized protein was dissociated by the injection of 400 mM imidazole (injection III), and chelated Ni(II) ions were removed by the injection of 200 mM EDTA (IV).

NTA moieties are engaged in the interaction with the H10-tag, thus increasing the multivalency of the interaction.

Improved Referencing by Selective Functionalization of Biacore Surfaces. One important application of ^{BT}tris-NTA is the possibility to convert commercially available streptavidin-functionalized substrates for selectively capturing His-tagged proteins. We tested different sensor chips for surface plasmon resonance detection. On a Biacore sensor chip SA, which is based on a dextran hydrogel layer, specific and highly stable immobilization of MBP-H10 was observed, which was reversible upon injection of imidazole (Figure 5).

The option to load ^{BT}tris-NTA on only one of the channels provides the possibility to obtain a reference channel without chelator head groups. Thus, the specificity of immobilization and subsequent binding experiments can be directly probed, in contrast to conventional NTA surfaces, where transition metal ion contamination impedes selective immobilization on a single channel. Thus, referencing enables for detecting EDTA binding to immobilized Ni(II) ions, followed by dissociation of the Ni(II) ions together with EDTA from the surface (cf. Figure 5, injection IV).

Multiplexed Protein Interaction Analysis by SPR Microarray Detection. We exploited the versatility opened by spatially resolved functionalization with ^{BT}tris-NTA using a multiplexed SPR platform provided by the ProteOn XPR36 system.

Here, a fluidic system based on 2 sets of 6 channels, which are perpendicularly crossing each other on the substrate, addresses 36 measurement spots at the junctions of the channels (Figure 6a). We explored specificity and activity using the well-characterized interaction of TEM1 lactamase with its protein inhibitor BLIP.[24] Different proteins with different His-tags were simultaneously immobilized onto the surface of the sensor chip, and binding of different analytes injected in different concentrations in the perpendicular direction was monitored. Immobilization curves obtained with BLIP-H10 in buffer and in crude *E. coli* lysate are compared in Figure 6b. Again, substantially lower levels of the H6-tagged protein as for the H10-tagged protein were observed. Very similar levels of stably immobilized proteins were obtained for BLIP-H10 injected in buffer and in a crude *E. coli* lysate. The functional properties of the immobilized proteins were probed by injecting the respective interaction partners. Because the complex of wild-type TEM1 and BLIP is very stable (k_d: ~1 $\times$ 10^{-4} s^{-1}), we applied the mutants TEM1 E104A and BLIP F142A, which dissociate from the respective wild-type counterpart with increased rate constants (k_d: 4 $\times$ 10^{-3} s^{-1} for TEM1 E104A and 1.5 $\times$ $10^{-2}s^{-1}$ BLIP F142A). Specific and fully reversible binding of the analyte at different concentrations confirmed the full activity of the immobilized proteins (Figure 6c,d). These measurements corroborated the highly specific capturing of His-tagged proteins directly from a complex protein matrix such as an *E. coli* lysate. The interaction rate constants obtained from monoexponential curve fitting were in excellent agreement with published data.[31] Studies of analyte binding signals over a prolonged period highlight the extremely stable tethering of the protein through the H10-tag: after a minor loss upon the first exposure of the analyte, the binding capacity of the immobilized protein remained constant over more than 16 h (Figure 6e).

Another feature enabled by in situ functionalization with ^{BT}tris-NTA in combination with versatile microfluidics is the pos-

(31) Reichmann, D.; Cohen, M.; Abramovich, R.; Dym, O.; Lim, D.; Strynadka, N. C.; Schreiber, G. *J. Mol. Biol.* **2007**, *365*, 663−679.

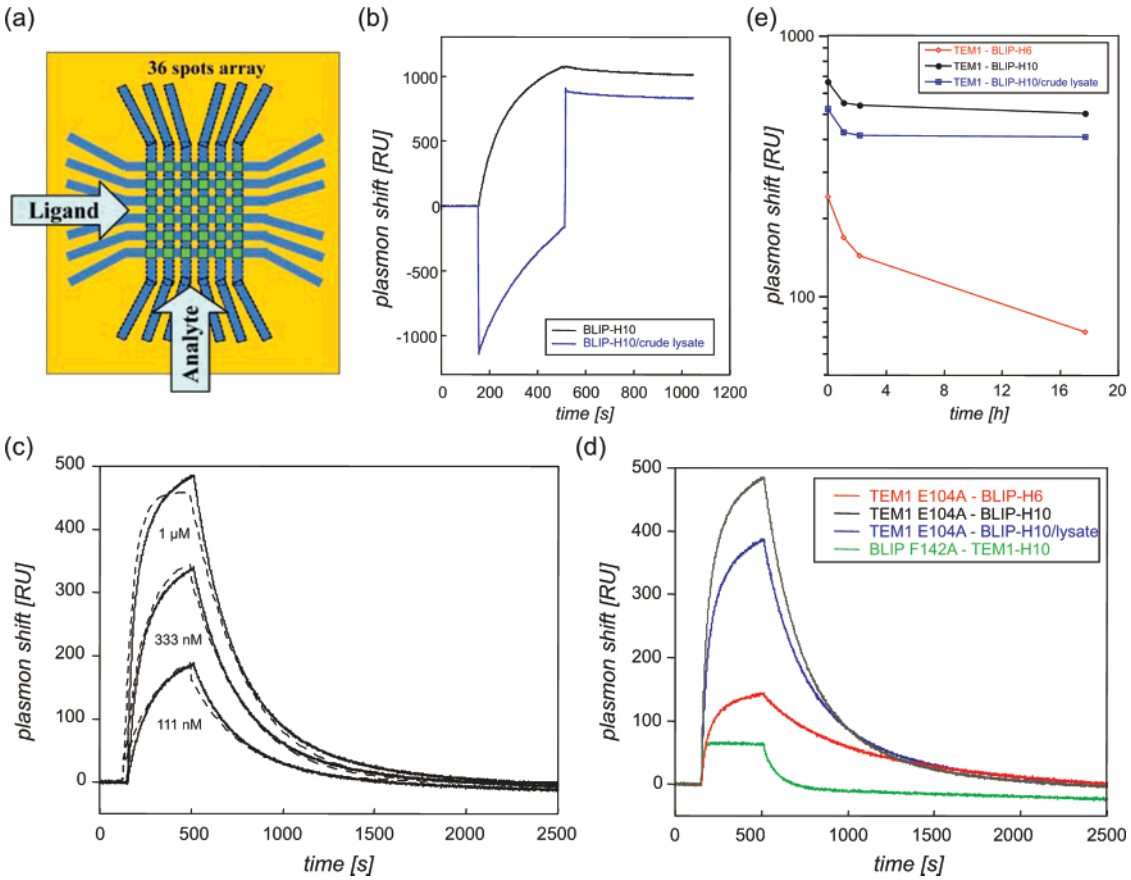

Figure 6. Multiplexed protein immobilization and protein interaction analysis. (a) Principle of the ProteOn XPR36 fluidics: an array of 36 spots is addressed by 2 perpendicular sets of 6 flow channels (blue). After loading of ^{BT}tris-NTA, four different His-tagged proteins (1 μM BLIP-H10, BLIP-H10 in crude *E. coli* lysate, BLIP-H6, and TEM1-H10) were captured on different channels. After 90° rotation of the chip, 6 analytes (TEM1 E104A: 1000, 333, and 111 nM. BLIP F142A: 2100, 700, and 233 nM) were injected in parallel. (b) Immobilization sensorgrams of BLIP-H10 in buffer and in crude *E. coli* lysate. The drop in the blue curve during injection is due to the different refractive index of the *E. coli* lysate. (c) Binding of TEM1 in three different concentrations to BLIP-H10 captured from buffer (solid line). The dashed line corresponds to a global fit of these data. (d) Comparison of the analyte binding signals of various combinations. (e) Stability of the surface loading after immobilization of BLIP-H10, BLIP-H6, and BLIP-H10 in crude lysate monitored over several hours by probing TEM1 binding.

sibility to control and vary the surface concentration of the immobilized protein by loading the streptavidin surface with different concentrations of ^{BT}tris-NTA. The injection scheme followed for this type of experiment is depicted in Figure 7a and b: After injection of ^{BT}tris-NTA in different concentrations, BLIP-H10, BLIP-H6, and TEM1-H10 are injected in perpendicular direction.

The analyte was injected in the same direction as the ^{BT}tris-NTA, thus simultaneously binding to the ligand at different surface concentrations. Indeed, different levels of immobilization were observed on the different spots in good correlation with the concentration of ^{BT}tris-NTA injected (Figure 7c,d). Again, analyte binding levels confirmed full activity of the immobilized ligands in good correlation with the amount of immobilized protein (Figure 7e,f). Fitting of the dissociation kinetics yielded dissociation rate constants of 3.5×10^{-3} s^{-1} for TEM1 E104A and 1.5×10^{-2} s^{-1} for BLIP F142A, which were essentially independent of the surface concentration of the immobilized ligand. Simultaneous interaction of the analyte with two or more immobilized ligands would substantially slow down the dissociation kinetics compared to a 1:1 interaction. The probability of simultaneous interaction with multiple immobilized ligands increases with the ligand density on the surface, confirming the 1:1 interaction between TEM and BLIP. Thus, simultaneous measurement of ligand binding kinetics at different surface densities enables identifying cooperative interactions in multi-protein complexes.[32]

Detection of Proteins in Complex Sample Matrixes. The highly specific and high-affinity recognition of His-tagged proteins by ^{BT}tris-NTA allows for protein labeling and detection in complex matrixes. Thus, we explored the specificity of labeling a His-tagged receptor in the plasma membrane of a living cell with streptavidin-functionalized quantum dots (Figure 8a). For this purpose, the ifnar2 subunit of the type I interferon receptor fused to an N-terminal H10-tag (H10-ifnar2) was transiently transfected into HeLa cells and biotinylated by addition of 100 nM ^{BT}tris-NTA for 15 min. Subsequently, streptavidin-conjugated QD655 was added, and the cells were imaged by confocal laser scanning microscopy. In parallel, OG488-labeled interferon α2 (^{OG488}IFNα2) was injected, which is a high-affinity ligand of ifnar2. Indeed, only those cells were labeled with QD 655 that also showed specific ligand binding (Figure 8a). Labeling occurred exclusively at the plasma membrane, confirming the integrity of the cells. However, internalization of the quantum dots was observed after some time, which was probably due to the high functionalization degree of the

(32) Klenkar, G.; Valiokas, R.; Lundström, I.; Tinazli, A.; Tampé, R.; Piehler, J.; Liedberg, B. *Anal. Chem.* **2006**, *78*, 3643−3650.

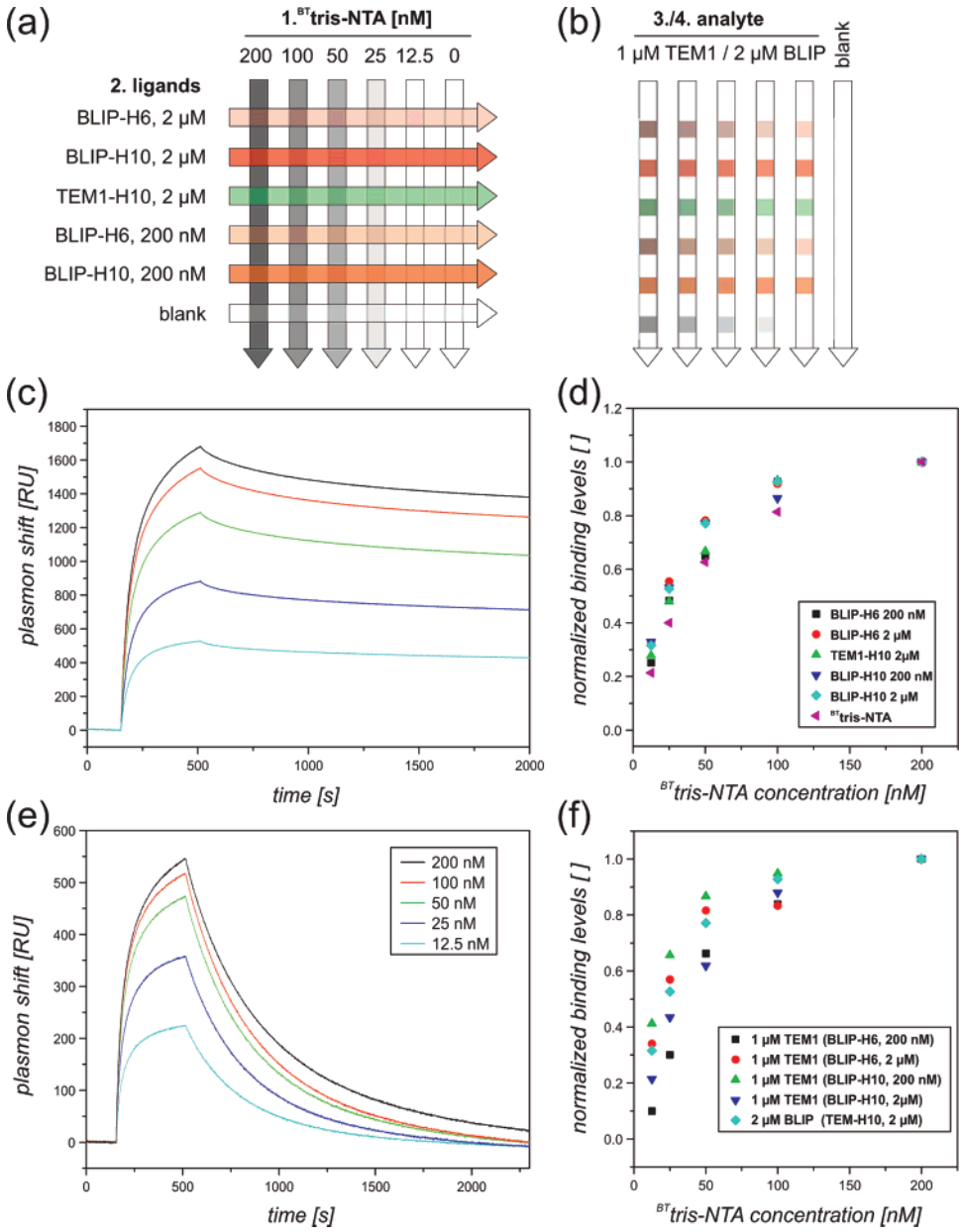

Figure 7. Parallel protein immobilization on a ^{BT}tris-NTA density array. (a, b) Scheme of the flow path used for functionalization with ^{BT}tris-NTA, protein immobilization, and analyte binding. (a) ^{BT}tris-NTA was injected at different concentrations in one direction, and different His-tagged proteins were immobilized in the orthogonal direction. (b) Subsequently, first 1 μM TEM1 E104A and then 2 μM BLIP F142A were injected on all channels orthogonal to the protein immobilization. (c) Sensorgrams observed for 2 μM BLIP-H10 at different concentrations of ^{BT}tris-NTA (according to the color coding indicated in the legend of panel e. (d) Summary of the immobilization levels observed on different channels as a function of ^{BT}tris-NTA concentration used for immobilization, normalized to the signals of the highest ^{BT}tris-NTA concentration. (e) Binding of TEM1 E104A to BLIP-H10 immobilized at 2 μM on ^{BT}tris-NTA at different concentrations. (f) Summary of the analyte binding levels observed on different channels as a function of ^{BT}tris-NTA concentration used for immobilization, normalized to the signals at the array element with the highest ^{BT}tris-NTA concentration.

quantum dots (20−25 streptavidin molecules per quantum dot), leading to cross-linking of the receptor subunit on the cell surface.

A further attractive application of ^{BT}tris-NTA is the detection of recombinant proteins by Western blot. While specific antibodies against the His-tag have been developed, a low molecular reagent for recognition of His-tags could considerably facilitate the procedure. In contrast to traditional mono-NTA, tris-NTA recognizes with high specificity the cumulated oligohistidines, which is a unique feature of the His-tag. For exploring the potency of ^{BT}tris-NTA for Western blot analysis, *E. coli* lysate doped with MBP-H6 and MBP-H10 in different concentrations were separated by SDS-PAGE. After electroblotting of the proteins onto a nitrocellulose membrane, 20 nM ^{BT}tris-NTA was incubated for 30 min followed by a streptavidin−HRP conjugate. Unambiguous detection down to 10 ng of MBP-H6 and 3 ng of MBP-H10 loaded onto the gel was achieved, while negligible nonspecific signals from the *E. coli* proteins were observed under these conditions. These results stress the high specificity of the interaction of tris-NTA with His-tagged proteins, enabling selective capturing, detection, and labeling of proteins in complex sample matrixes.

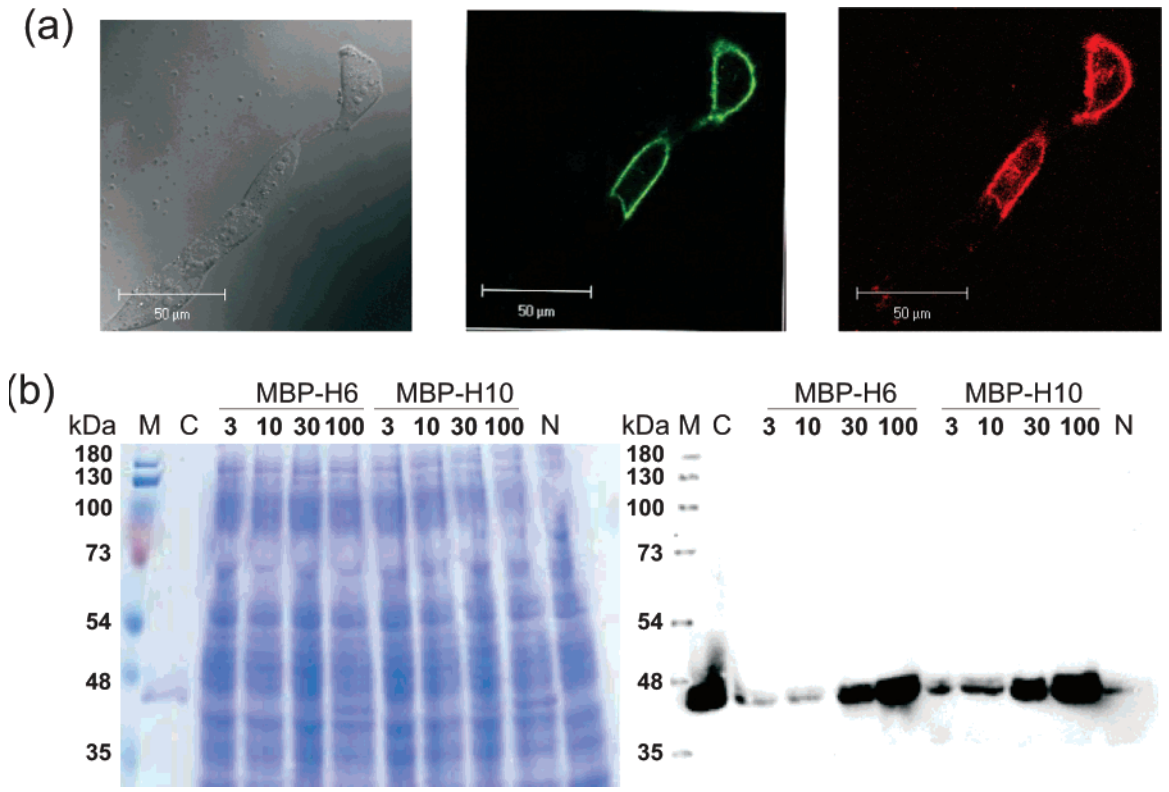

Figure 8. Protein detection in complex matrixes. (a) Selective quantum dot labeling of ifnar2 with a N-terminal His-tag expressed on the surface of live cells as detected by confocal fluorescence microscopy. After biotinylation with ^{BT}tris-NTA, strepavidin-functionalized quantum dots QD655 were added, followed by ^{OG488}IFNα2. Left, transmission image; center, green fluorescence from the ^{OG488}IFNα2; right, red fluorescence from QD655). (b) Detection of MBP-H10 and MBP-H10 at different concentrations in crude *E. coli* lysate by Western blot analysis. Left, image of the Commassie-stained gel; right, image of the Western blot developed with ^{BT}tris-NTA and streptavidin/horsh radish peroxidase conjugate visualized by enhanced chemiluminescence. (M, marker; C, positive control, 100 ng purified MBP-H10; 3, 10, 30, and 100, amount of protein (in ng) loaded in each lane; N, negative control, bacterial lysate.

CONCLUSIONS

We have here introduced ^{BT}tris-NTA as a novel tool for reversible biotinylation of His-tagged proteins. We could show that streptavidin functionalized with ^{BT}tris-NTA binds His-tagged proteins with a stoichiometry of 1:1 and 1:2. It seems that the His-tagged protein—in particular the H10-tag—involves two tris-NTA moieties simultaneously, leading to an even increased binding affinity compared to individual tris-NTA/H10 interaction. Though we cannot exclude that steric constraints also contribute to the strict limitation, it seems that simultaneous engagement of two tris-NTA by one His-tag is in itself energetically favorable. We have already observed a similar phenomenon on density arrays of multivalent chelator heads, which we termed "surface multivalency".[33] Thus, the distance between the adjacent biotin binding sites of streptavidin in combination with the rather long linker between the tris-NTA and the biotin moieties apparently permits simultaneous interaction with a single His-tag.

Using different schemes of conjugations, we have demonstrated the versatility of ^{BT}tris-NTA for bioanalytical application. The high affinity of the tris-NTA/oligohistidine complexes permits highly stable, yet reversible biotinylation of His-tagged proteins, thus enabling selective capturing of recombinant proteins from complex sample matrixes directly to streptavidin-functionalized substrates. This scheme provides the utmost specificity, as tris-NTA in solution only recognizes highly cumulated histidines.[16] While the captured proteins remained bound to streptavidin for days, these complexes are readily cleaved by imidazole or histidine under physiological pH and ionic strength. A further advantage of this scheme is the comparably fast association of the biotin—streptavidin complex, making it possible to efficiently capture His-tagged proteins even at low concentrations. Alternatively, by reaction with ^{BT}tris-NTA, streptavidin can be efficiently converted into a carrier with high affinity for His-tagged proteins. Using commercial biosensor systems with multichannel microfluidics, spatially resolved functionalization of the streptavidin surface with tris-NTA in variable concentrations was demonstrated. Selective functionalization with ^{BT}tris-NTA and a defined stoichiometry of the interaction with His-tagged proteins eliminates the key drawback of conventional NTA surfaces: because a high density of NTA groups is required for stable immobilization of His-tagged proteins, the excess NTA-complexed Ni(II) ions frequently cause strong nonspecific binding. Furthermore, spatially resolved surface functionalization with ^{BT}tris-NTA provides versatile schemes for multiplexed binding assays including density variation of immobilized proteins and negative controls. Moreover, His-tagged proteins can be immobilized to the sensor chip directly from the crude lysate, shortening significantly the time needed to set up such experiments. Thus, ^{BT}tris-NTA provides a powerful means for conjugating the His-tag world to the (strept)avidin world. The broad availability of (strept)avidin-functionalized substrates for

(33) Valiokas, R.; Klenkar, G.; Tinazli, A.; Tampé, R.; Liedberg, B.; Piehler, J. *Chembiochem* **2006**, *7*, 1325−1329.

almost any bioanalytical technique on the one hand and the broad usage of the His-tag on the other ensures countless possibilities for future application of ^{BT}tris-NTA.

ACKNOWLEDGMENT

J.P. thanks Gerhardt Spatz-Kümpel for excellent technical assistance, and Robert Tampé for hosting and supporting the group. This project was supported by grants to J.P. from the Deutsche Forschungsgemeinschaft (Emmy-Noether Program PI 405/1, PI 405/2, and SFB628), and by the BMBF (0312005A) and to G.S. by grant 8525 from Minerva.

Received for review July 14, 2007. Accepted September 5, 2007.

AC0714922